Int. J. Exp. Path. (2010), 91, 72–86
doi: 10.1111/j.1365-2613.2009.00670.x

ORIGINAL ARTICLE

Perforin-expressing cytotoxic cells contribute to chronic cardiomyopathy in *Trypanosoma cruzi* infection

Jaline Coutinho Silverio*, Luzia Maria de-Oliveira-Pinto*, Andréa Alice da Silva*,†, Gabriel Melo de Oliveira‡ and Joseli Lannes-Vieira*

*Laboratório de Biologia das Interações, Instituto Oswaldo Cruz, Fiocruz, Rio de Janeiro, Brazil, †Departamento de Patologia, UFF, Niterói, Brazil and ‡Laboratório de Biologia Celular, Instituto Oswaldo Cruz, Fiocruz, Rio de Janeiro, Brazil

INTERNATIONAL JOURNAL OF EXPERIMENTAL PATHOLOGY

Summary

Understanding the dual participation of the immune response in controlling the invader and at the same time causing tissue damage might contribute to the design of effective new vaccines and therapies for Chagas disease. Perforin, a cytolytic protein product of killer cells, is involved in resistance to acute *Trypanosoma cruzi* infection. However, the contribution of perforin in parasite control and chronic chagasic cardiomyopathy is unclear. Perforin-positive cells were detected in the heart tissue during the acute and chronic phases of infection of C57BL/6 mice inoculated with low dose (10^2 parasites) of the Colombian *T. cruzi* strain. This protocol led to acute phase survival in both wild-type and perforin null ($pfp^{-/-}$) mice lineages. During the chronic infection, parasitism and inducible nitric oxide synthase (iNOS) as well as interleukin (IL)-4^+ and, mainly, interferon (IFN)-γ^+ cells were more elevated in the heart tissue of $pfp^{-/-}$ mice. Higher levels of circulating NO and anti-parasite immunoglobulin (Ig)G2c and IgG3, paralleled by a prominent frequency of IFN-γ^+ and IL-10^+ splenocytes, were present in $pfp^{-/-}$-infected mice. Therefore, although the perforin-dependent pathway plays a role, it is not crucial for anti-*T. cruzi* immunity and acute phase survival of mice infected with a low inoculum. Further, perforin deficiency resulted in lower activity of creatine kinase-muscle brain isoform (CK-MB) isoenzyme in serum and a more restricted connexin 43 loss, both of which are markers of the cardiomyocyte lesion. Moreover, perforin deficiency hampered the development of severe electrocardiographic abnormalities. Hence, our results corroborate that perforin-bearing cytotoxic cells might contribute to cardiomyocyte lesion and heart dysfunction during chronic *T. cruzi* infection, shedding light on immunopathogenesis of chronic chagasic cardiomyopathy.

Keywords
cardiomyopathy, $CD8^+$ T-cells, Chagas disease, cytokines, perforin, *Trypanosoma cruzi*

Received for publication:
2 November 2008
Accepted for publication:
2 April 2009

Correspondence:
Joseli Lannes-Vieira
Laboratório de Biologia das Interações
Instituto Oswaldo Cruz
Fiocruz
Av. Brasil 4365
Rio de Janeiro 21045-900
Brazil
Tel.: +55-21 3865 8202
Fax: +55-21-2209-4110
E-mail: lannes@ioc.fiocruz.br

Jaline Coutinho Silverio and Luzia Maria de-Oliveira-Pinto contributed equally to this study.

Trypanosoma cruzi is the causative agent of Chagas disease, an affliction that results in debilitating heart disease in 30–40% of the infected individuals, contributing significantly to morbidity and mortality in South America (Higuchi *et al.* 2003; Marin-Neto *et al.* 2007). Chagasic cardiomyopathy is mainly characterized by prominent inflammation associated with fibrosis and electrical dysfunction (Higuchi *et al.* 2003). Although autoimmunity has been ascribed to explain the immunological attack of host tissues, the most accepted conjecture is that cardiac injury results from unbalanced effector immune responses that are elicited by persistent parasites (Higuchi *et al.* 2003; Kierszenbaum 2005). Therefore, the comprehension of how the immune response controls the invader, although inflicting heart tissue damage, poses a challenge to design effective vaccines and new therapies for Chagas disease.

$CD8^+$ T-cells are the major cell population in the heart tissue of chronic cardiomyopathic chagasic patients (Reis *et al.* 1993; Higuchi *et al.* 1997). Considering the functional role of heart-infiltrating $CD8^+$ T-cells, there is a good correlation between the numbers of interferon (IFN)-γ^+ cells and $CD8^+$ T-cells of chagasic patients presenting successful parasite control (Reis *et al.* 1997). In corroboration, the role of IFN-γ-producing $CD8^+$ T-cells in *T. cruzi* dissemination control has been well documented in experimental models (Martin & Tarleton 2004; Tzelepis *et al.* 2007). Conversely, the presence of heart-infiltrating granzyme A-expressing $CD8^+$ cytotoxic T lymphocytes (CTL) is associated with severity of cardiac dysfunction in chronic chagasic patients (Reis *et al.* 1993). These findings led us to propose that at least part of the heart-infiltrating $CD8^+$ T-cells, acting as CTL, are involved in tissue damage during chronic Chagas disease (Lannes-Vieira 2003; Marino *et al.* 2004); however, this hypothesis remains poorly supported.

Perforin-mediated cytolysis is a crucial effector mechanism in CTL (Pipkin & Lieberman 2007). Nevertheless, studies approaching the role of CTL in *T. cruzi* infection adopting perforin-deficient infected mice are controversial. Mice with disruption in perforin or granzyme B genes had parasitaemia and mortality rates similar to wild-type animals and were protected from secondary infection by prior exposure to avirulent parasites, indicating that either perforin- or granzyme B-mediated lytic pathways are not required for *T. cruzi* control (Kumar & Tarleton 1998). Conversely, perforin-dependent cytolytic mechanisms clearly play a major role in resistance to acute *T. cruzi* infection, this contribution perhaps being strain and challenge dose-dependent (Nickel & Sharma 2000). Although heart parasitism and parasitaemia were similar, perforin-deficient mice infected with the Y strain of *T. cruzi* exhibited more intense myocarditis, cardiomyocyte destruction and cumulative mortality than their infected counterparts (Henriques-Pons *et al.* 2002). In addition, mice lacking perforin as well as both A and B granzymes infected with the highly pathogenic *T. cruzi* strain Tulahuen succumbed earlier and at a higher rate than C57BL/6 wild-type mice, indicating that these lytic pathways are crucial for acute infection control (Muller *et al.* 2003).

In the present study, adopting the Colombian strain model of *T. cruzi*-elicited chronic myocarditis and cardiomyopathy (dos Santos *et al.* 2001; Garcia *et al.* 2005; Medeiros *et al.* 2009), we first demonstrated the presence of perforin-expressing cells among the heart-infiltrating cells. These results led us to address the participation of perforin in both parasite control and immunopathogenesis of *T. cruzi*-triggered chronic cardiomyopathy.

Materials and methods

Animals

Five- to seven-week-old female C57BL/6 (H-2^b) and perforin-deficient ($pfp^{-/-}$, B6.129-pfp-^{tm1Clrk}-) mice from the Oswaldo Cruz Foundation (Fiocruz, Rio de Janeiro, Brazil) animal facilities were maintained under specific pathogen free (SPF) conditions. Perforin-deficient C57BL/6 mice resulted of seven back-crossings of the original perforin-deficient lineage (Walsh *et al.* 1994) in C57BL/6 mice. All mice were manipulated according to institutional guidelines for animal ethics of Fiocruz (CQB/CTNBio-105/99, CEUA-Fiocruz-161/03).

Experimental infection

Mice were infected intraperitoneally with 10^2 blood trypomastigotes of the *T. cruzi* Colombian strain isolated from a cardiac chagasic patient (Federici *et al.* 1964) and maintained by serial passages from mouse to mouse. Parasitaemia was estimated from 5 μl of tail vein blood, the detection of rare trypomastigotes marking the onset of the chronic phase as previously described (Federici *et al.* 1964; dos Santos *et al.* 2001).

Reagents and antibodies

For immunohistochemistry staining (IHS), the polyclonal antibody recognizing *T. cruzi* antigens was produced in our laboratory (LBI/IOC-Fiocruz, Brazil). Purified anti-F4/80 antigen (clone F4/80) antibody was purchased from CALTAG Laboratories (Burlingame, CA, USA). Supernatants were home-made with anti-mouse CD8a (53–6.7) and

anti-mouse CD4 (GK1.5) hybridomas. In our IHS studies, monoclonal antibodies, anti-mouse perforin (CB5.4; Alexis Biochemicals, Plymouth Meeting, PA, USA), anti-IFN-γ (R4-6A2; BD PharMingen, San Jose, CA, USA) and anti-interleukin (IL)-4 (BVDG-24G2; CALTAG) as well as the purified polyclonal antibody recognizing inducible nitric oxide synthase (iNOS) from mouse macrophages (RAW 264.7; Cayman Chemical, Ann Arbor, MI, USA) were applied; the polyclonal antibody recognizing connexin 43 was purchased from Sigma (St. Louis, MO, USA); the biotinylated anti-rat immunoglobulin (Ig) from DAKO (Glostrup, Denmark) and the biotinylated anti-rabbit immunoglobulin and peroxidase–streptavidin complex from Amersham (England). Appropriate controls were prepared by replacing primary antibodies with purified rat immunoglobulin or normal rabbit serum.

For flow cytometry studies, AlloPhycoCyanin (APC)-conjugated anti-mouse CD4 (GK1.5), Fluorescein isothiocyanate (FITC)-conjugated anti-mouse CD8a (clone 53-6.7), Phycoerythrin (PE)-conjugated anti-mouse IFN-γ (XMG1.2) and PE-anti-mouse IL-4 (11B11) were purchased from BD PharMingen (USA) and PE-anti-IL-10 (RM9104) from CALTAG (USA). Appropriate controls were prepared by replacing primary antibodies with the respective isotypes. Alkaline phosphatase-conjugated goat anti-mouse IgG1, IgG2c or IgG3 were obtained from Southern Biotechnology (La Jolla, CA, USA) for the enzyme-linked immunosorbent assay (ELISA) assays.

Immunohistochemistry

Groups of 8–10 infected and 3–5 age-matched, non-infected control mice were killed under anaesthesia at various time points after infection. The hearts were removed, embedded in tissue-freezing medium (Tissue-Tek; Miles Laboratories, Nutley, NJ, USA) and stored in liquid nitrogen for IHS. Serial cryostat sections, 5 μm thick, were fixed in cold acetone and subjected to indirect immunoperoxidase staining, as previously described (dos Santos *et al.* 2001). For negative controls, heart tissue sections from experimentally infected mice were submitted to all the steps of the reaction excluding the addition of the primary antibodies. Sections of spleen were adopted as positive controls for lymphocyte staining. The numbers of $CD4^+$, $CD8^+$, $F4/80^+$, IFN-γ^+ and IL-4^+ inflammatory cells were counted in 50 microscopic fields (10×25 magnification) per section. Perforin staining was performed according to the manufacturer's instructions. The numbers of perforin-positive cells were counted in 50 microscopic fields (10×40 magnification) per section. The expression of *T. cruzi*, iNOS and connexin-43 positive areas in heart tissue sections was also evaluated with a digital morphometric apparatus. The images were analysed with AnaliSYS Program, so that the areas expressing and non-expressing the studied molecules could be integrated. Fifty fields per section, in three sections per heart, were analysed. The percentage of positive area for the studied molecules was measured in 50 fields (25 mm^2).

Parasite-specific IgG1, IgG2c and IgG3 by ELISA

In order to detect anti-*T. cruzi*-specific IgG1, IgG2c and IgG3, the plates (Nalge Nunc International, Rochester, NY, USA) were coated overnight at 4 °C with 10 μg/ml of total *T. cruzi* antigens prepared as previously described (Michailowsky *et al.* 2001) in 0.05 M phosphate buffer followed by blockage with 2% albumin in phosphate buffer saline (PBS) for 2 h at 37 °C. Serum from individual animals was diluted 1/20 in PBS with 1% albumin–0.05% Tween 20 (PBST) and incubated for 2 h at 37 °C and 1 h at 4 °C. Alkaline phosphatase-conjugated goat anti-mouse IgG1, IgG2c or IgG3 diluted 1/1000 in PBST was added to each well and the plate was incubated overnight at 4 °C. The assay was developed with the para-nitrophenol phosphate of sodium substrate (Sigma-Aldrich, St. Louis, MO, USA), and the reaction was stopped with 3 M sodium hydroxide solution and read at 405 nm.

NO quantification

Nitrate and nitrite were determined in serum as previously described (Miranda *et al.* 2001). The nitrite concentration in serum was assayed with a microplate by mixing 50 μl of serum with 50 μl of Griess reagent and the A_{540} was read 15 min later. The concentration of nitrate was determined with the addition of Vanadium III solution followed by a 30 min incubation at 37 °C, 5% CO_2 and 90% humidity, 90 min after which the A_{540} was read. The NO_2^- and NO_3^- concentrations were then determined by reference to a standard curve of 0.8–200 μM of $NaNO_2$ and $NaNO_3$.

Cell preparation and intracellular cytokine staining by flow cytometry analysis (FACS)

The animals were killed by blood draining under anaesthesia, and harvested spleens were teased into single cell suspensions as previously described (dos Santos *et al.* 2001). Splenocytes were incubated with 5 μg/ml of brefeldin A (Sigma) during 4 h at 37 °C. The cells were collected, washed, resuspended in PBS containing 2% fetal calf serum and labelled as described (dos Santos *et al.* 2001). Controls

of specific labelling were prepared with isotype-matched antibodies. One-colour labelled samples were prepared to set compensation values. Samples were acquired with a FACScalibur (Becton Dickinson, Franklin Lakes, NJ, USA), gating the mononuclear cells and using a narrow forward-angle light scatter parameter to exclude dead cells from the analysis. At least 20,000 cells were acquired inside this gate. Fluorescence gates were cut in accordance with the labelling controls, respecting curve inflexions. The FACS was carried out with the Summit v.4.3 Build 2445 program (Dako, Carpinteria, CA, USA).

IFN-γ and IL-4 enzyme-linked immunospot (ELISpot) assays

The ELISpot assay for enumeration of IFN-γ and IL-4 producing cells was performed essentially as previously described (Miyahira *et al.* 1995). Our assays were conducted with anti-mouse IFN-γ (R4-6A2; BD PharMingen) or IL-4 (BVD4-1D11; BD PharMingen) antibodies diluted in PBS (5 μg/ml) in triplicates and incubation of antigen presenting cells primed with total *T. cruzi* antigens (10 μg/ml) for 30 min at 37 °C. Concanavalin A (ConA; 5 μg/ml) was applied as mitogenic stimulation. After incubation, freshly isolated splenocytes from experimental animals were seeded at a suspension of 5×10^5 cells/well and incubated for 20 h at 37 °C and 5% CO_2. Either biotin-conjugated anti-mouse IFN-γ (clone XMG1.2, BD PharMingen) or IL-4 (clone BVD6-24G2, BD PharMingen, USA) was used to detect the captured cytokines. Alkaline phosphatase-labelled streptavidin (BD PharMingen, USA) followed by nitro blue tetrazolium (NBT, Sigma, USA) plus 5-Bromo-4-chloro-3-indolyl phosphate (BCIP, Sigma, USA) dissolved in Tris buffer (0.9% NaCl, 1% $MgCl_2$, 1.2% Tris in H_2O) were applied to reveal the spots. The mean of spot numbers in triplicate wells was obtained for each condition, and the number of specific IFN-γ and IL-4-secreting T-cells was calculated by stimulated spot count/10^6 cells. The assay was read with the CTL OH-ImmunoSpot® A3 Analyzer model (USA).

Creatine kinase (CK) detection

The activity of CK-MB isoenzyme, one of myocardial injury marker, was measured with commercial kits (Labtest, Lagoa Santa, MG, Brazil) as previously described (de Souza *et al.* 2000). Incubation of sera samples with the substrate led to a net increase in NADPH concentration, directly proportional to the enzyme activity in the samples. The assay was adapted for reading in a microplate spectrophotometer (Microplate Reader Benchmark; Bio-Rad, Memphis, TN, USA) to allow the study of small quantities of mouse serum according to the manufacturer's recommendation. The optical density at 340 nm was recorded every 2 min for 15 min.

Electrocardiographic (ECG) records

All mice were intraperitoneally tranquilized with diazepan (20 mg/kg) and transducers were carefully placed subcutaneously according to chosen preferential derivation (DII). Traces were recorded with a digital system (Power Lab 2/20) connected to a bio-amplifier in 2 mV for 1 s (PanLab Instruments, Barcelona, Spain). Filters were standardized between 0.1 and 100 Hz, and traces were analysed with the Scope software for Windows V3.6.10 (PanLab Instruments, Holliston, MA, USA). We measured heart rate (beats per minute, bpm), duration of the PR, QRS, QT intervals and P wave in milliseconds (ms) on the 150th day postinfection (dpi). The relationship between the QT and RR intervals in the mouse was assessed in all animals. To obtain physiological relevant values for the heart rate-corrected QT interval (QT_c) in units of time (rather than time to a power not equal to 1), the observed RR interval (RR_0) was first expressed as a unitless multiple of 100 ms, this yielding a normalized RR interval, $RR_{100} = RR_0/100$ ms. Next, the value of the exponent (y) in the relationship $QT_0 = QT_c \times RR^y_{100}$ was assessed, where QT_0 is the observed QT (in ms), units for QT_c also being milliseconds, taking the natural logarithm of each side of this relationship $[(QT_0) = \ln (QT_c) + y \ln(RR_{100})]$. Thus, the slope of the linear relationship between the log-transformed QT and RR_{100} defined the exponent to which the RR interval ratio should be raised to correct QT for heart rate (Mitchell *et al.* 1998).

Statistical analysis

Data were expressed as arithmetic mean ± SD. Student's *t*-test was adopted to analyse the statistical significance of the apparent differences. The Kaplan–Meier method was employed to compare survival rates of the studied groups. All statistical tests were performed with SPSS 8.0 software. Differences were considered statistically significant at $P < 0.05$.

Results

Perforin-expressing cells are detected in the heart of acutely and chronically Trypanosoma cruzi-infected C57BL/6 mice

As expected, perforin-positive cells were found neither in the heart tissue of non-infected C57BL/6 controls (Figure 1a)

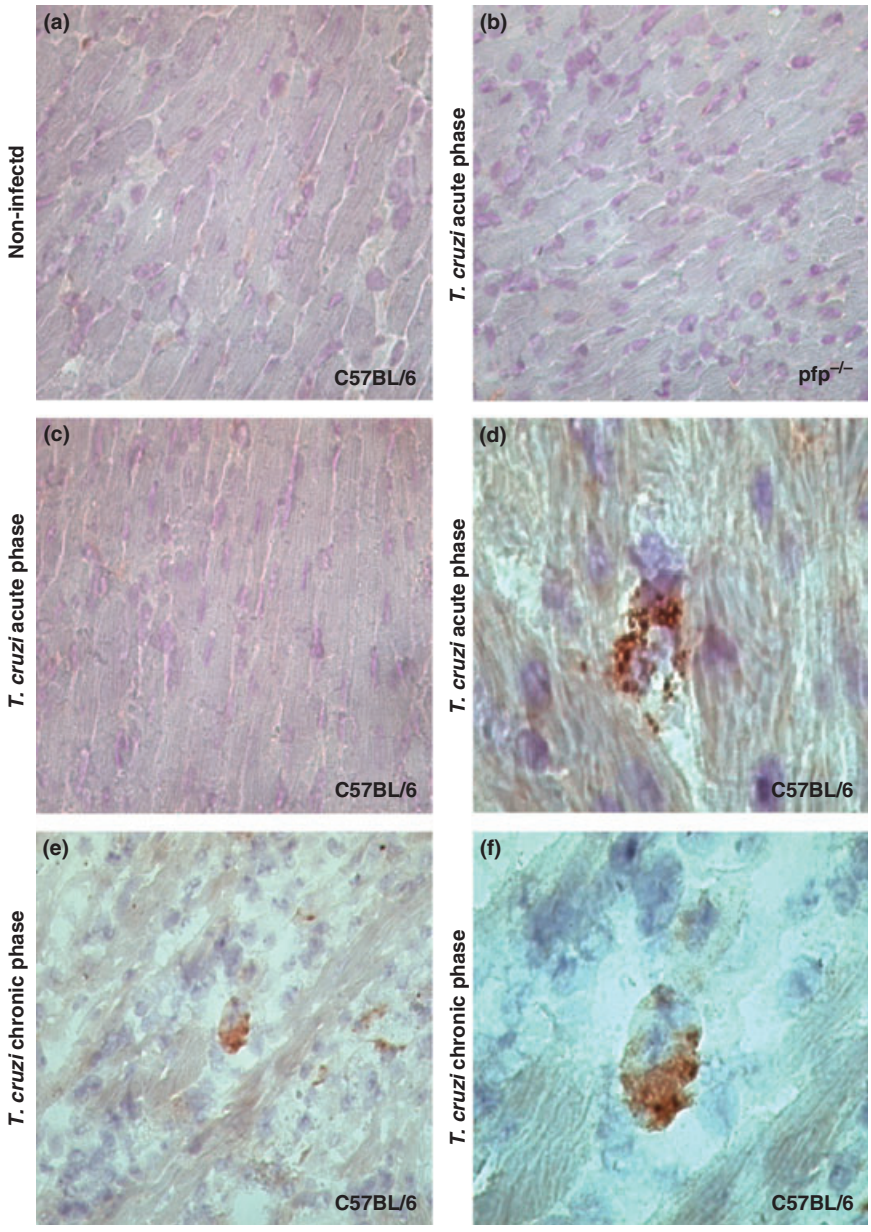

Figure 1 Immunohistochemical staining (IHS) for perforin in heart tissue of C57BL/6 and pfp$^{-/-}$ mice. The figure shows representative pictures of IHS detection of perforin in the heart tissue sections of (a) non-infected C57BL/6 mouse, (b) *Trypanosoma cruzi*-infected pfp$^{-/-}$, (c) *T. cruzi*-infected C57BL/6 in absence of the primary anti-perforin antibody and (d) *T. cruzi*-infected C57BL/6 mice at day 50 postinfection. (e) and (f) are representative heart tissue sections from infected C57BL/6 mice at day 150 postinfection. Perforin-expressing cells are mononuclear cells and perforin is not restricted to the cytoplasm but released onto the adjacent cardiomyocytes (d, arrows head). Panels a, b, c and e, 400×; panels d and f, 1000×. Each experimental group consisted of four analysed mice, in two independent experiments.

nor in pfp$^{-/-}$ mice (Figure 1b). Further, there was no positive staining for perforin in the heart sections from infected C57BL/6 in the absence of the primary antibody (Figure 1c). Perforin-expressing cells were detected in the cardiac tissue of *T. cruzi*-infected C57BL/6 mice during the acute (50 dpi) and chronic (150 dpi) phases (Figure 1d–f). Interestingly, perforin staining was not restricted to the cytoplasm of the infiltrating mononuclear cells (Figure 1e,f) but was of granular nature and was apparently released onto the adjacent cardiomyocytes (Figure 1d). Perforin-positive cells were also detected in the spleen during both the acute and chronic infection (data not shown).

Perforin is not crucially required for Trypanosoma cruzi dissemination control and acute phase survival

Initially, in order to determine the role of perforin in *T. cruzi* infection control, parasitaemia and survival were assessed in perforin-deficient and C57BL/6 wild-type mice infected with 10^2 parasites. There was increased parasitaemia (Figure 2a) and parasitism (Figure 2c,d) in *T. cruzi*-infected pfp$^{-/-}$ mice in comparison with C57BL/6 at 50 dpi, reinforcing the participation of perforin signalling in resistance to acute *T. cruzi* infection. In most of the experiments, 100% of the C57BL/6 and pfp$^{-/-}$-infected

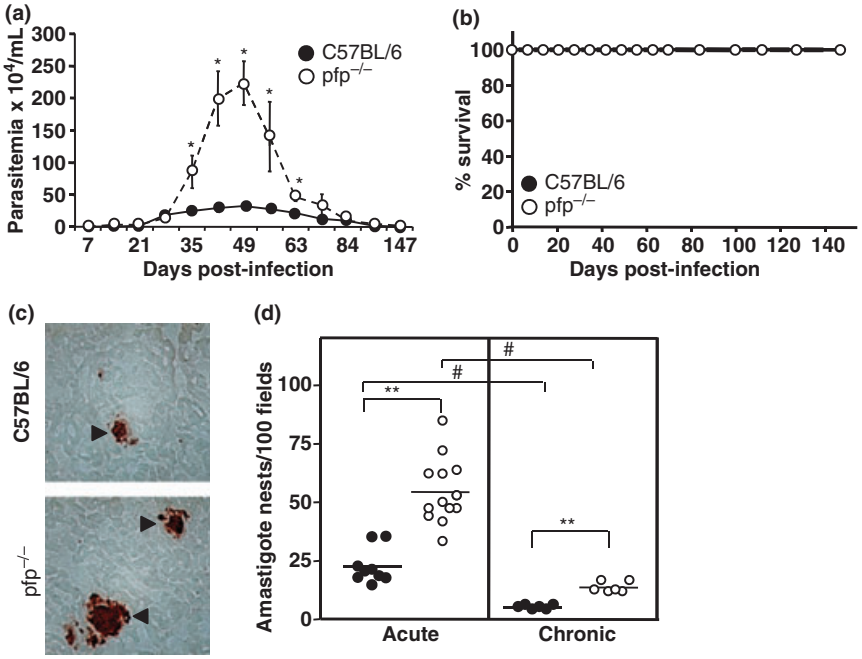

Figure 2 Parasitaemia, survival curves and heart parasitism of C57BL/6 and pfp$^{-/-}$ mice infected with 10^2 blood trypomastigote forms of the Colombian strain of *Trypanosoma cruzi*. The parasitaemia (a) and survival curves (b) of C57BL/6 (black circle) and pfp$^{-/-}$ (white circle) *T. cruzi*-infected mice are shown. Mean ± SD values for 7–10 mice per group are shown and data are representative of three independent experiments. (c) Heart tissue sections from C57BL/6 and pfp$^{-/-}$ mice at 50 days postinfection show amastigote-positive staining (red, arrows head). Original magnification is 400×. (d) Numbers of amastigote nests in 100 histological fields of cardiac sections obtained from C57BL/6 (black circle) or pfp$^{-/-}$ (white circle) mice at acute (50 days postinfection) and chronic (150 days postinfection) phases of infection. Each value represents an individual mouse. This represents three independent experiments. $^*P < 0.05$ and $^{**}P < 0.01$, comparing wild-type *vs.* pfp$^{-/-}$ *T. cruzi*-infected mice; $^{\#}P < 0.01$, comparing the acute *vs.* chronic phases of infection.

mice survived (Figure 2b). In the late stage of infection (150 dpi), no parasite burden was apparent in either group of *T. cruzi*-infected mice. Further, during the chronic phase in both wild-type and pfp$^{-/-}$ groups, heart parasitism was significantly reduced in comparison with the acute phase, although significant and persistent increased parasitism was observed in infected pfp$^{-/-}$ mice (Figure 2d).

iNOS expression in the cardiac tissue and NO levels in serum are upregulated in perforin absence

Considering that pfp$^{-/-}$ mice infected with the Colombian strain survived the acute infection progressing to the chronic phase, we addressed the putatively involved mechanisms in parasite control in these mice. In the acute infection (50 dpi), there was a higher expression of iNOS in the heart tissue of pfp$^{-/-}$ as compared with the wild-type mice. Regardless of the decrease in iNOS expression in the chronic phase (150 dpi), pfp$^{-/-}$ animals still presented higher iNOS expression than C57BL/6 (Figure 3a,b). In line with this, we questioned whether or not the absence of perforin could affect NO production ability, a mechanism required to eliminate *T. cruzi*. In all infected mice, NO levels in serum were higher compared with the non-infected mice. The amounts of NO at 50 dpi were significantly greater in pfp$^{-/-}$ mice compared with the wild-type C57BL/6 animals. However, there was no statistical difference when comparing the levels of NO in pfp$^{-/-}$ and C57BL/6 in the chronic *T. cruzi* infection (Figure 3c).

Upregulation of antibody and cytokine production in perforin-deficient mice

To further analyse the involved mechanisms in parasite control in the absence of perforin, we assessed the production of specific anti-*T. cruzi* antibodies. As exhibited in Figure 4, *T. cruzi*-specific IgG1 production was not severely affected by perforin deficiency; however, pfp$^{-/-}$-infected mice displayed an increased production of specific anti-*T. cruzi* IgG2c and IgG3 antibodies compared with the wild-type C57BL/6 mice (Figure 4a).

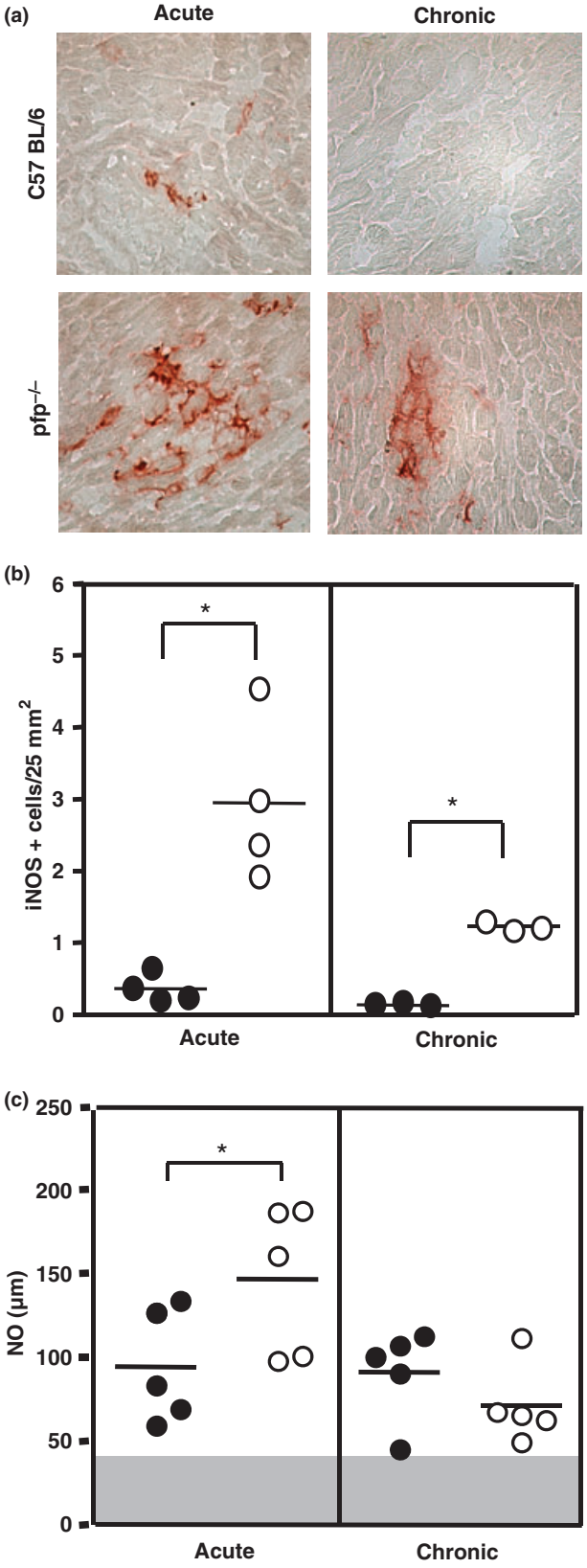

We set out to understand the dynamics of Th1 and Th2 cytokine production considering that IFN-γ producers (Th1) are involved in resistance while IL-4 producers (Th2) are involved in susceptibility to *T. cruzi* infection (Kumar & Tarleton 2001). In the acute phase, a substantial fraction of region 1 gated splenocytes (R1), mainly composed of T-cells, produced these cytokines in both groups of infected animals. Moreover, the *ex vivo* IFN-γ production by R1 splenocytes from *T. cruzi*-infected pfp$^{-/-}$ mice was markedly accentuated compared with the wild-type infected mice (Figure 4b). There was an increased IL-4 basal level in non-infected pfp$^{-/-}$ mice in comparison with the non-infected C57BL/6 mice. Further, IL-4 and IL-10 expression was upregulated in *T. cruzi*-infected pfp$^{-/-}$ and C57BL/6 mice in comparison with the non-infected mice (Figure 4b). Moreover, the production of the regulatory cytokine IL-10 was upregulated in pfp$^{-/-}$ compared with the wild-type *T. cruzi*-infected mice (Figure 4b).

In order to identify the functional capacity of the T-cells generated in both pfp$^{-/-}$ and C57BL/6 *T. cruzi*-infected mice, IFN-γ- and IL-4-secreting splenocytes specific to *T. cruzi* antigens or responding to mitogen stimulation were assessed by adopting the ELISpot assay (Table 1). More impressive differences appeared upon IFN-γ- and IL-4-secreting cells to mitogen in non-infected C57BL/6 mice compared with those infected. In contrast, analysis of the IFN-γ ELISpot response to mitogen revealed a higher frequency of responders among pfp$^{-/-}$-infected mice than those non-infected, while IL-4-secreting cells were much more prominent in the non-infected pfp$^{-/-}$ mice. A consistent difference was observed in the IFN-γ-secreting cells to *T. cruzi* antigens in both C57BL/6 and pfp$^{-/-}$-infected mice compared with the non-stimulated cells. Moreover, compared with the wild-type

Figure 3 Immunohistochemistry analyses of inducible nitric oxide synthase (iNOS)-expressing cells in the heart tissue and NO levels in serum of *Trypanosoma cruzi*-infected mice. (a) Representative pictures of iNOS$^+$ cells in heart tissue sections of *T. cruzi*-infected C57BL/6 and pfp$^{-/-}$ mice at 50 (acute) and 150 (chronic) days postinfection. (b) The number of iNOS$^+$ cells in 25 mm^2 of area of cardiac tissue sections obtained from C57BL/6 (black circle) or pfp$^{-/-}$ (white circle) mice at acute (50 days postinfection) and chronic (150 days postinfection) phases are shown. Each circle represents an individual mouse. The data represent two independent experiments. (c) NO_2^- plus NO_3^- levels were determined in the serum during the acute and chronic phases of infection. The graphs show means of five animals per group. The data are representative of two independent experiments. The grey area represents the mean plus twofold SD of non-infected mice for NO levels in serum. *$P < 0.05$ for comparison of pfp$^{-/-}$ (white circle) *vs.* C57BL/6 (black circle) infected mice at the same time point.

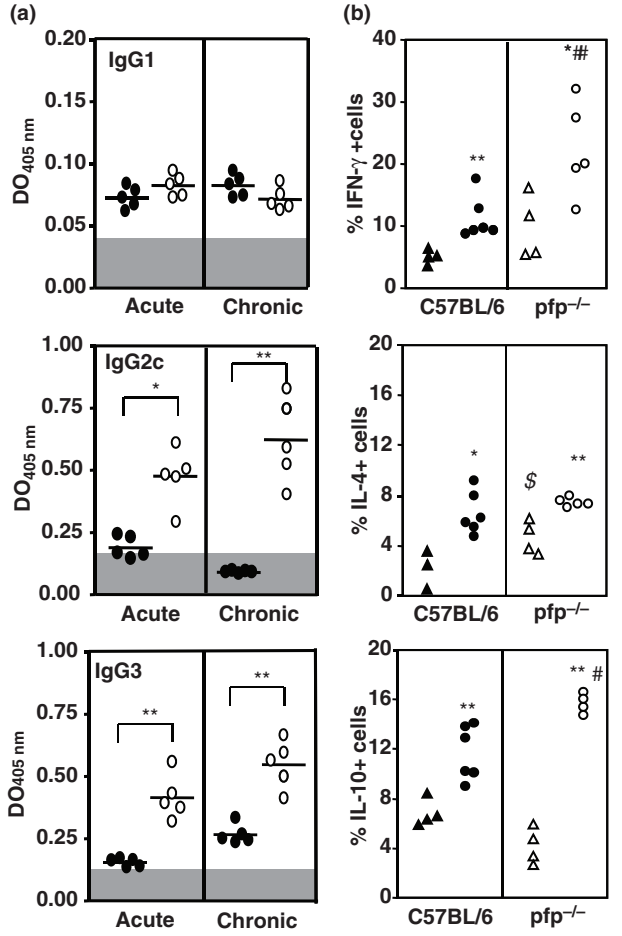

Figure 4 Expression of antibodies and cytokines is upregulated in pfp$^{-/-}$ and C57BL/6 mice during *Trypanosoma cruzi* infection. (a) Profile of antibody levels in serum of infected C57BL/6 and pfp$^{-/-}$ mice. Anti-*T. cruzi* lysate immunoglobulin (Ig)G1, IgG2c and IgG3 isotypes were determined in the serum during the acute and chronic phases of infection. The graphs show means of at least five animals per group. The data are representative of two independent experiments. The gray area represents the mean plus twofold SD of non-infected mice for each IgG isotype. $^{*}P < 0.05$ or $^{**}P < 0.01$ for comparison of pfp$^{-/-}$ (white circle) *vs.* C57BL/6 (black circle) infected mice at the same time point. (b) Splenocytes from non-infected (triangles) or *T. cruzi*-infected (circles) C57BL/6 (black) and pfp$^{-/-}$ (white) mice were incubated *in vitro* with Brefeldin A. After 4 h of incubation, the cells were harvested and cytokine production was evaluated by intracellular staining. Averages of 3–6 mice per group are presented in total lymphocytes (R1 gate) that produce interferon-γ, interleukins 4 and 10. The data represent one out of two-three experiments. Non-infected *vs.* infected, $^{*}P < 0.05$ or $^{**}P < 0.01$; infected *vs.* infected, $^{\#}P < 0.05$; non-infected *vs.* non-infected, $^{\$}P < 0.05$.

Table 1 Detection of interferon (IFN)-γ- and interleukin (IL)-4-producing T-cells in early infection by *Trypanosoma cruzi*

	Medium	ConA (5 μg/ml)	*T. cruzi* antigens (10 μg/ml)
IFN-γ SFC/10^6 cells			
C57BL/6 NI	24 ± 15	889 ± 553†	–
C57BL/6 50 dpi	69 ± 47	426 ± 107†	125 ± 35*‡
pfp$^{-/-}$ NI	17 ± 3	193 ± 78†	–‡
pfp$^{-/-}$ 50 dpi	60 ± 21	528 ± 158	259 ± 113**‡
IL-4 SFC/10^6 cells			
C57BL/6 NI	24 ± 15†	896 ± 563†	–
C57BL/6 50 dpi	63 ± 52†‡	426 ± 107†	239 ± 120**
pfp$^{-/-}$ NI	156 ± 44†‡	4391 ± 2398†	–
pfp$^{-/-}$ 50 dpi	157 ± 38‡	440 ± 60	170 ± 52

$^{*}P < 0.05$ or $^{**}P < 0.01$, medium *vs. T. cruzi* antigens.
$^{\dagger}P < 0.05$, non-infected *vs.* non-infected.
$^{\ddagger}P < 0.05$, infected *vs.* infected.
NI, non-infected.

mice absence of perforin affords IFN-γ upregulation in *T. cruzi*-infected mice (Table 1).

Perforin deficiency protects mice from Trypanosoma cruzi*-induced* chronic cardiac tissue damage

Subsequent to cell lesion, membrane integrity is lost, macromolecules being diffused to extracellular spaces and drained into blood vessels. The evaluation of the cardiac CK-MB isoenzyme, a marker of myocardial injury, revealed significant increase in the activity of this isoenzyme in the serum of *T. cruzi*-infected C57BL/6 mice in the acute and, particularly, during the chronic infection (Figure 5a). During the acute infection, intense inflammatory infiltrates were detected in the heart tissue of *T. cruzi*-infected C57BL/6 wild-type mice. However, there was a reduction in the numbers of cells invading the cardiac tissue during the chronic phase of infection (Figure 5b), indicating that myocardial injury is neither related to the intensity of inflammation (Figure 5b) nor to the parasite load (Figure 2d) during the chronic phase of infection.

To investigate whether the increased production of IFN-γ and IL-4 in *T. cruzi*-infected wild-type mice was compartmentalized to secondary immune tissue (Figure 4b) or broadly found, we assessed the expression of these cytokines in the heart tissue. Similar to what was detected in the spleen, there was a significant accumulation of IFN-γ- and IL-4-producing cells in the target organ during the acute infection. In addition, both IFN-γ^{+} and IL-4^{+} cell

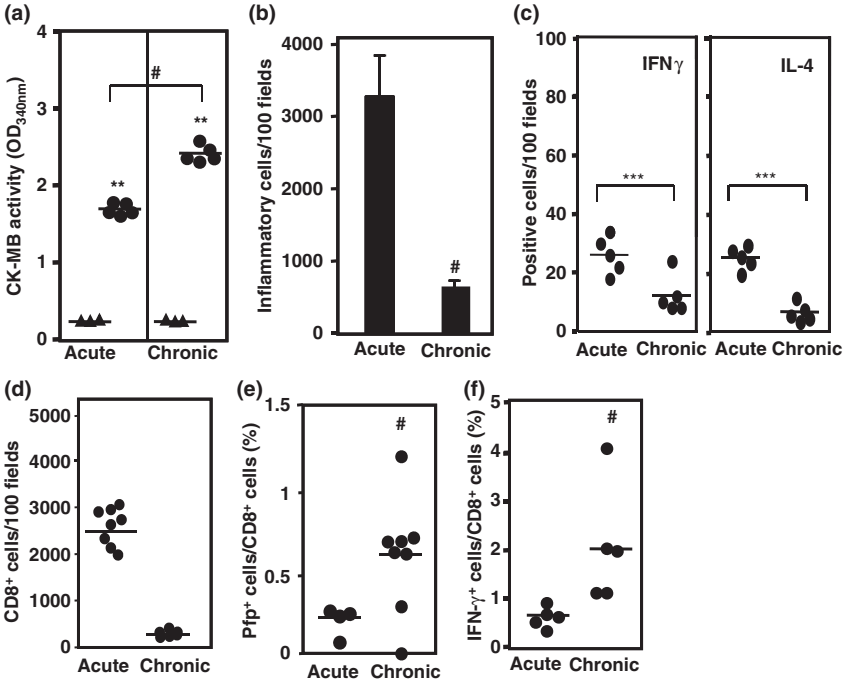

Figure 5 Cardiomyocyte damage and inflammatory cells in the heart tissue of acute (50 days postinfection) and chronically (150 days postinfection) *Trypanosoma cruzi*-infected C57BL/6 mice. (a) Cardiomyocyte lesion was evaluated by creatine kinase cardiac isoenzyme MB (CK-MB) activity in serum samples from C57BL/6 mice (black circle) in comparison with the non-infected controls (black triangle). $CD8^+$, perforin-positive, interferon (IFN)-γ^+ and interleukin (IL)-4^+ cells were immunohistochemically analysed in serial sections of heart tissue. (b) Total inflammatory mononuclear cells in the cardiac tissue of infected mice. (c) IFN-γ^+ and IL-4^+ as well as (d) $CD8^+$ cells invading heart tissue during *T. cruzi* infection. The relative frequency of (e) perforin-positive or (f) IFN-γ^+ cells among $CD8^+$ cells in the heart tissue of acute and chronically infected mice was estimated. At least 200 fields (four sections per analysed mouse) were counted for each parameter at each time point studied. Each value represents an individual mouse. $^{**}P < 0.01$ or $^{***}P < 0.001$ comparing non-infected *vs.* *T. cruzi*-infected mice; $^{\#}P < 0.01$ comparing the acute *vs.* the chronic phases of infection.

populations shrank as the infection progressed and the chronic phase was established (Figure 5c).

Trafficking of $CD8^+$ immunocompetent T-cells contributes to *T. cruzi*-elicited myocarditis formation in chagasic patients and experimental models. Even among $CD8^+$ effector cells, evidence is emerging that subpopulations may be present, having diverse capability to destroy target cells and secrete IFN-γ (Sandberg *et al.* 2001). Employing IHS analysis, the frequency of $CD8^+$ T-cells and the relative frequency of perforin-positive and IFN-γ^+ cells among $CD8^+$ cells infiltrating the cardiac tissue was evaluated during *T. cruzi* infection using serial sections of heart tissue. Although double labelling was not performed, we assumed that most of the perforin-positive cells were $CD8^+$ CTL as the frequency of NK cells was 0.5–1% of the inflammatory cells and there was coincidental positioning of perforin/cytokine expression and $CD8^+$ cells in serial sections. There was a significant accumulation of $CD8^+$ cells in the heart tissue of acutely *T. cruzi*-infected mice, which diminished during the chronic infection (Figure 5d). Interestingly, increased ratios of perforin-positive/$CD8^+$ invading cells (Figure 5e) were detected in the cardiac tissue of C57BL/6 mice in the chronic infection. Similar results appeared when IFN-γ^+/$CD8^+$ cells (Figure 5f) were analysed. Considering the reduction in the numbers of inflammatory cells invading the heart tissue during the chronic infection phase, our data indicate that an enrichment in IFN-γ^+ and perforin-positive cells occurs in this tissue as the infection evolves (Figure 5e,f).

To directly approach the participation of perforin-positive and IFN-γ^+ cells in *T. cruzi*-elicited chronic cardiomyopathy, $pfp^{-/-}$ mice were infected with 10^2 blood trypomastigotes of the Colombian strain. Increased numbers of IFN-γ- and IL-4-producing cells were detected in the cardiac tissue of chronically infected $pfp^{-/-}$ mice when compared with C57BL/6-infected mice (Figure 6a). Further, during the chronic phase of infection (150 dpi), the numbers of inflammatory mononuclear cells increased in the heart of $pfp^{-/-}$ mice in comparison with C57BL/6 mice (1635 ± 321

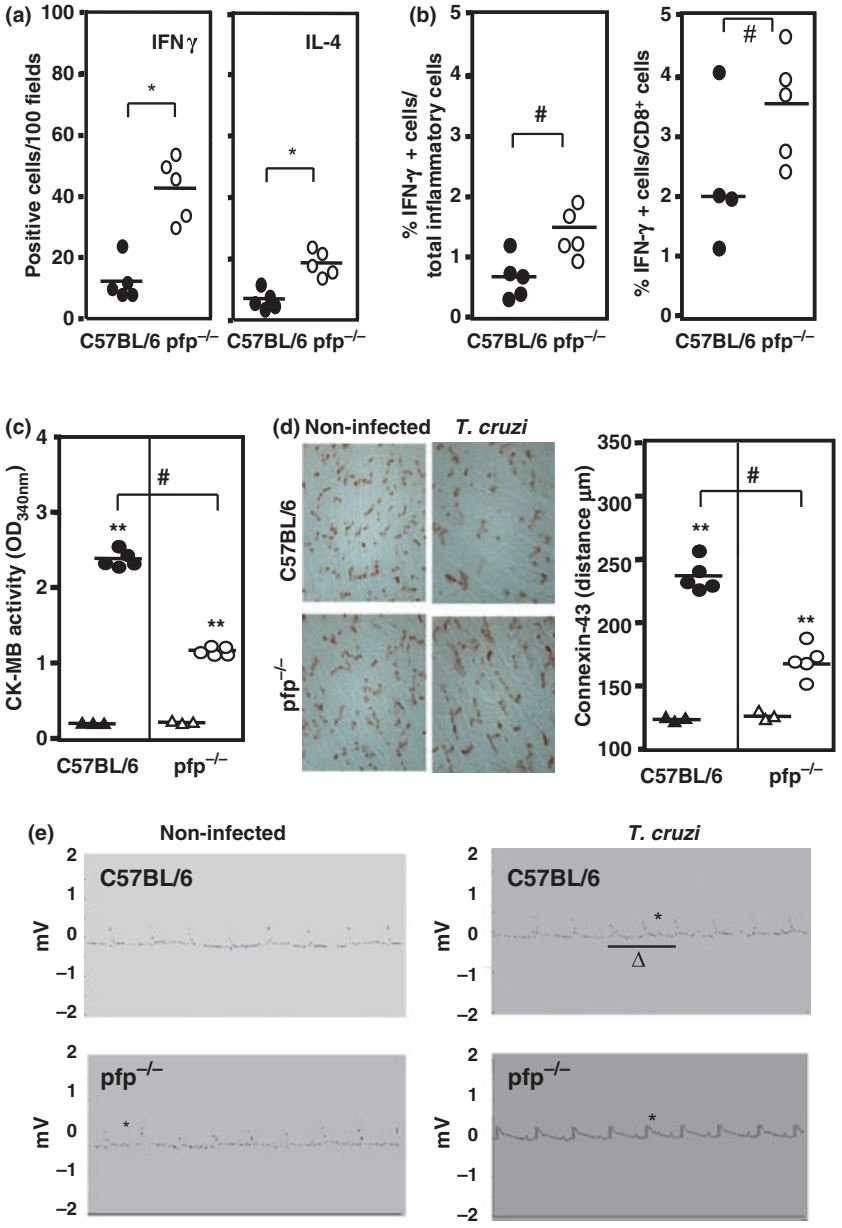

Figure 6 The presence of inflammatory interferon (IFN)-γ^+ and interleukin (IL)-4^+ cells in the cardiac tissue and heart damage characterized by creatine kinase cardiac isoenzyme MB (CK-MB) activity in serum, loss of connexin 43 and electrocardiographic (ECG) abnormalities in C57BL/6 and pfp$^{-/-}$ mice at 150 days postinfection. (a) IFN-γ^+ and IL-4^+ cells invading heart tissue during chronic *Trypanosoma cruzi* infection. (b) The relative frequencies of IFN-γ^+ cells among total inflammatory mononuclear cells and $CD8^+$ cells are shown. (c) Cardiomyocyte damage was evaluated by CK-MB activity in serum samples from chronically infected C57BL/6 (black circle) and pfp$^{-/-}$ (white circle) mice in comparison with the non-infected mice (black/white triangles). (d) The pattern of connexin 43 characterizing intercalary discs of cardiomyocytes was analysed in non-infected and chronically infected C57BL/6 and pfp$^{-/-}$ mice. Quantification of the distance between intercalary discs of cardiomyocytes revealed as connexin 43 cluster labelling in *T. cruzi*-infected C57BL/6 (black circle) and pfp$^{-/-}$ (white circle) mice in comparison with the non-infected mice (black/white triangles). Each value represents an individual mouse. The data are representative of two or three experiments. (e) ECG recordings from non-infected and *T. cruzi*-infected C57BL/6 and pfp$^{-/-}$ mice; * and Δ represent second-degree atrioventricular block and sinusal arrhythmia respectively. Representative records from 5–10 analysed animals per group. $^{**}P < 0.01$comparing non-infected *vs.* *T. cruzi*-infected mice; $^{\#}P < 0.01$ comparing the wild-type *vs.* the pfp$^{-/-}$ *T. cruzi*-infected mice.

Table 2 Electrocardiographic analysis of non-infected and *Trypanosoma cruzi*-infected mice

Experimental group	Heart rate (no. of beats/minute)	PR interval (ms)	*P*-wave duration (ms)	QRS complex (ms)	QT interval (ms)	QT_c
C56BL/6 NI ($n = 5$)	508.0 ± 56.1	35.9 ± 1.3	12.1 ± 0.7	11.7 ± 1.2	22.2 ± 0.7	20.2 ± 1.4
C57BL/6 150 dpi ($n = 10$)	418.0 ± 42.1*	55.5 ± 12.2*	14.0 ± 2.3	9.7 ± 1.0	24.2 ± 5.1	20.2 ± 2.2
$pfp^{-/-}$ NI ($n = 5$)	432.0 ± 26.4	38.2 ± 6.4	11.8 ± 3.6	11.5 ± 1.8	30.8 ± 5.5	26.1 ± 2.7
$pfp^{-/-}$ 150 dpi ($n = 5$)	436.8 ± 96.4	34.6 ± 7.8†	12.6 ± 3.2	9.9 ± 2.1	32.6 ± 1.7	27.9 ± 3.1

*$P < 0.05$, infected *vs.* non-infected.
†$P < 0.01$, wild-type infected *vs.* $pfp^{-/-}$ infected.
dpi, days postinfection.

cells/100 fields in $pfp^{-/-}$ mice *vs.* 916 ± 170 cells/100 fields in C57BL/6 mice; $P < 0.05$). Chronically infected $pfp^{-/-}$ mice presented higher frequencies of IFN-γ^+ cells/total heart inflammatory cells and, more remarkably, higher frequencies of IFN-γ^+ cells/$CD8^+$ T-cells in comparison with C57BL/6 wild-type mice (Figure 6b).

Inspection of CK-MB isoenzyme activity on 150 dpi revealed that $pfp^{-/-}$-infected mice had lower CK-MB levels as compared with the C57BL/6-infected mice (Figure 6c). To further assess the cardiac function, immunolocalization of connexin 43, a protein mainly responsible for electrical synchrony of cardiomyocytes (Severs *et al.* 2006), was evaluated in the myocardium of $pfp^{-/-}$ and C57BL/6 mice. There was an abundant expression of connexin 43 marking gap junctions in clusters at the intercalary discs in the heart tissue from C57BL/6 and $pfp^{-/-}$ non-infected controls (Figure 6d). In contrast, in the late phase of infection (150 dpi) a substantial reduction in connexin 43 expression associated with abnormal organization and enhancement of distance in the connexin labels was detected in heart tissue from C57BL/6 mice, being less pronounced in $pfp^{-/-}$ chronically infected mice, somewhat resembling the pattern in hearts from non-infected animals (Figure 6d).

Perforin deficiency prevents the development of severe ECG abnormalities in chronic Trypanosoma cruzi infection

To further explore the participation of perforin in *T. cruzi*-elicited cardiac dysfunction, ECG analyses were carried out in chronically *T. cruzi*-infected wild-type and $pfp^{-/-}$ mice. Electrocardiographic abnormalities, such as bradycardia and increased PR interval, were frequent among the wild-type-infected mice compared with the non-infected age-matched mice (Figure 6e and Table 2). These abnormalities indicate a delay in the conduction of electric impulse together with an increase in the duration of ventricular action potential. Interestingly, the ECG of 80% of the wild-type infected mice depicted a 2° AVB (atrioventricular block) and in 40% a sinusal arrhythmia was found, suggesting bradycardia and delay in electric impulse conduction. More importantly, perforin deficiency protected infected mice from developing bradycardia and an increased PR interval (Figure 6e and Table 2).

Discussion

In Chagas disease, cardiomyopathy progression is related to persisting myocarditis (Higuchi *et al.* 2003; Marin-Neto *et al.* 2007), nevertheless how the immune response controls the invader but inflicts heart tissue damage remains a challenge. In the present work, for the first time the presence of perforin-positive cells in the cardiac tissue of *T. cruzi*-infected mice was demonstrated. Hence, we carried out a study to distinguish the differential contribution of the perforin-mediated pathway in *T. cruzi* control and chronic cardiomyopathy formation adopting perforin-deficient mice. Contrasting with studies involving the infection of $pfp^{-/-}$ mice with high inoculum of the Y strain or highly virulent *T. cruzi* strain (Nickel & Sharma 2000; Henriques-Pons *et al.* 2002; Muller *et al.* 2003), $pfp^{-/-}$ mice injected with a low inoculum of the *T. cruzi* Colombian strain survived the acute infection, which progressed to a chronic cardiomyopathy. Both wild-type and $pfp^{-/-}$-infected mice presented decreased parasitaemia and heart parasitism from the acute to the chronic phase, although higher numbers of parasite nests have still been detected in the heart tissue of $pfp^{-/-}$ mice in the late phase of infection. These data suggest that perforin plays a role in early parasite growth control, yet not influential neither in the late phase of infection nor for host survival.

To identify effector pathways acting in *T. cruzi* control in perforin absence, first we analysed *in situ* cardiac expression of iNOS as well as NO levels in serum of infected mice. In comparison with wild-type C57BL/6, higher expression of iNOS was detected in the heart tissue of $pfp^{-/-}$ mice during the acute infection persisting in the chronic phase, although to a lesser extent. Inducible nitric oxide synthase expression is related to detrimental effects in a non-infection cardiopathic condition (Feng *et al.* 2001). Similarly, iNOS expression in heart tissue was correlated with severity of myocarditis and cardiomyopathy in Brazil strain-infected mice (Huang *et al.* 1999). The participation of iNOS in *T. cruzi* resistance is controversial (Michailowsky *et al.* 2001; Cummings & Tarleton 2004); however, induced NO was consensually implicated in *T. cruzi* growth control in cardyomyocytes *in vitro* (Machado *et al.* 2000; Fichera *et al.* 2004). Accordingly, NO plays a role in parasitism control in the early acute *T. cruzi* infection (Michailowsky *et al.* 2001) but neither in the late acute nor the chronic infection (Saeftel *et al.* 2001). Our data show a burst of NO in serum restricted to the acute infection in $pfp^{-/-}$ compared with the wild-type mice, although to a lesser extent increased NO levels are still detected in both $pfp^{-/-}$ and wild-type chronically infected mice. In chronic chagasic patients, high NO levels in serum were associated with anti-oxidant imbalance and cardiomyopathy severity (Perez-Fuentes *et al.* 2003). Altogether, our results imply that in Colombian-infected $pfp^{-/-}$ mice, iNOS and NO might be a 'double-edged sword' contributing to parasite control yet participating in cardiac lesion, as these animals survived the acute infection but developed heart pathology, although less severe than the wild-type mice.

To further approach effector pathways implicated in *T. cruzi* control in $pfp^{-/-}$ mice, we analysed the levels of specific anti-*T. cruzi* antibodies as well as production of cytokine *ex vivo* and after antigen stimulation. Specific IgG1 production was not affected by perforin deficiency; however, higher parasite-specific IgG2c and IgG3 levels were apparent in $pfp^{-/-}$ in comparison with C57BL/6 infected mice, particularly during chronic infection. These antibodies may participate in *T. cruzi* control during chronic infection but might also indicate a continuous and long-lasting B-cell stimulation by persisting antigens and possibly contribute to lesion formation (d'Imperio Lima *et al.* 1986). Nevertheless, correlation between clinical forms or severity of Chagas disease and *T. cruzi*-speficic IgG isotype levels remains unsolved (Cordeiro *et al.* 2001; Michailowsky *et al.* 2003).

An incremental accumulation of IFN-γ-producing cells and IFN-γ-secreting cells in response to *T. cruzi* antigens were more apparent in the spleen of infected $pfp^{-/-}$ mice in comparison with C57BL/6. In *T. cruzi* infection, protective immunity depends critically on IFN-γ (Michailowsky *et al.* 2001). IFN-γ, combined with tumour necrosis factor, induces high levels of NO, primarily responsible for parasite replication control (Silva *et al.* 2003). ELISpot responses to a parasite lysate revealed that IFN-γ status inversely correlates with Chagas disease severity (Laucella *et al.* 2004). Further, the IL-10 upregulation detected in *T. cruzi*-infected $pfp^{-/-}$ compared with the wild-type mice might lead to a more balanced immune response hence a less severe pathology, as recently suggested by IL-10 polymorphism studies in chagasic patients (Costa *et al.* 2009). Interestingly, the perforin-mediated pathway is proposed to downregulate the immune response by way of limiting the antigen-presenting function (Sambhara *et al.* 1998). Whether or not the increased production of IFN-γ and IL-10 in *T. cruzi*-infected $pfp^{-/-}$ mice is either a result of the absence of the downregulatory role of perforin or a consequence of the amplified stimuli by increased parasitism in these mice still remains to be clarified. However, our findings suggest that IFN-γ and IFN-γ-inducible effector mechanisms (iNOS, NO, specific IgG isotypes) are responsible for parasite replication control and acute phase survival in *T. cruzi*-infected $pfp^{-/-}$ mice. Therefore, there is an inference that during *T. cruzi* infection the perforin-mediated pathway might be detrimental for effector immunity.

We demonstrated an inherited increase in IL-4 production by splenic cells from naïve $pfp^{-/-}$mice, to our knowledge the first time ever described. Further, IL-4 expression was upregulated during *T. cruzi* infection in both wild-type and $pfp^{-/-}$ mice. IL-4 administration prior to infection increased *T. cruzi* uptake and killing by macrophages (Wirth *et al.* 1989). Moreover, IL-4 presence during the initial activation of dendritic cells instructs naïve CD4 T-cells towards Th1 immunity (Biedermann *et al.* 2001). Accordingly, we propose that the substantial IL-4 production in $pfp^{-/-}$ naïve mice might be positively influential in Th1 potential, resulting in the increased IFN-γ expression detected during *T. cruzi* infection in $pfp^{-/-}$ mice. IL-4 has also been implicated in preventing B-cell apoptosis and allowing the maintenance of the B-cell pool (Foote *et al.* 1996). In this regard, the more prominent IL-4 levels prior to infection in $pfp^{-/-}$ mice might rescue parasite-specific B-cells, consequently enhancing circulating antibody levels, thereby favouring parasite control and infection chronification.

In C57BL/6 mice infected with the Colombian strain, although inflammation shrank as infection coursed from the acute to the chronic phase, cardiomyopathy evolved associated with increased frequency of perforin-positive and IFN-γ^+ cells among the heart-infiltrating cells. The ability of peripheral blood and heart-infiltrating $CD3^+CD4^+$ cells to produce IFN-γ has been related to cardiomyopathy in

T. cruzi-infected patients (Abel *et al.* 2001; Gomes *et al.* 2003). In contrast, production of IFN-γ by circulating $CD8^+$ cells has been linked with protection in reinfected and chronic patients with severe cardiomyopathy (Laucella *et al.* 2004). Similarly, IFN-$\gamma^{-/-}$ mice are less resistant to *T. cruzi* infection than their wild-type counterparts (Michailowsky *et al.* 2001). Our present findings support that the presence of IFN-γ^+ cells among the heart-invading cells in wild-type and, specially, in $pfp^{-/-}$-infected mice might be beneficial. It remains to be elucidated whether the protective role of IFN-γ is achieved by preventing parasite burden and/or protecting cardiomyocytes from inflammatory mediator-induced damage. Furthermore, our data indicate that susceptibility to myocardial dysfunction is a perforin-dependent process. Although presenting increased parasitism, $iNOS^+$ and IFN-γ^+ cells as well as myocarditis, $pfp^{-/-}$ mice demonstrated better preserved heart tissue, which is revealed with decreased CK-MB release and restricted loss of connexin 43, reinforcing the participation of pfp^+ cells in heart lesion. Differential cell accumulation of $iNOS^+$ and IFN-γ^+ in the cardiac tissue of Met-RANTES-treated chronically infected mice also led to a more preserved connexion 43 expression and diminished CK-MB levels (Medeiros *et al.* 2009). Further, in comparison with the wild-type animals, $pfp^{-/-}$-infected mice present a more regular cardiac electric conduction, probably reflecting better preservation of sinusal nodes and atrioventricular function (Garcia *et al.* 2005), reinforcing the participation of perforin in cardiomyopathy pathogenesis. It was claimed that the perforin-mediated pathway does not play a role in direct lysis of cardiomyocytes in $pfp^{-/-}$ infected with the Y strain that succumbed to the acute infection (Henriques-Pons *et al.* 2002). In contrast, a decrease in CK-MB was also observed, in adopting the Colombian strain, during the acute infection in $pfp^{-/-}$ mice (data not shown). In addition, cardiomyocyte lesion is aggravated during the chronic infection of C57BL/6 mice when the ratio of perforin-positive/total inflammatory cells and perforin-positive/$CD8^+$ infiltrating cells in the heart tissue is enhanced, further supporting the involvement of $CD8^+$ CTL, acting via the perforin pathway, in Chagas cardiomyopathy. In this context, although suggested by the detection of cytotoxic lymphocytes infiltrating the heart tissue in several cardiomyopathies and *in vitro* experiments, the contribution of perforin-mediated cytotoxicity in cardiac conditions *in vivo* has not been firmly established (Binah 2002). To our knowledge, this is the first time that the participation of perforin in heart tissue damage in an *in vivo* model of cardiomyopathy induced by a chronic infection has ever been described.

In conclusion, we offer evidence that killer cells acting via perforin are not essential for anti-*T. cruzi* immunity but might be key players in cardiomyocyte lesion and heart dysfunction, providing support for a pathophysiological mechanism involved in chronic chagasic cardiomyopathy generation. Thus, further studies evaluating the precise participation of perforin and perforin-related or regulated molecules will pave the way to the understanding of chronic chagasic cardyomyopathy, possibly disclosing new therapeutic strategies.

Acknowledgements

The authors are grateful to Dr Belmira dos Santos for breeding the $pfp^{-/-}$ mice and Ms. Marilene Damazio dos Santos and Mrs Luiz Carlos da Silva for their excellent technical assistance. Also, the authors are in debt to Dr Ana Paula Marino and MSc Márcia Terra for collecting blood and tissue samples. English review and revision by Mitchel Raymond Lishon (UCLA, USA) is also acknowledged.

This work was supported in part by grants from FAPERJ (E-26/171.126/2005; E-26/111.756/2008) and the Brazilian Research Council/CNPq (Universal #471518/2006-7; DECIT #410401/2006-4; National Institute for Science and Technology – INCT/CNPq/2008). L. M. de-Oliveira-Pinto and J. Lannes-Vieira are research fellows of the CNPq. The authors have no relevant financial interests related to this manuscript, including employments, consultancies, honoraria, stock ownerships or options, expert testimony, grants or patents received or pending, or royalties.

References

Abel L.C., Rizzo L.V., Ianni B. *et al.* (2001) Chronic Chagas' disease cardiomyopathy patients display an increased IFN-gamma response to *Trypanosoma cruzi* infection. *J. Autoimmun.* **17**, 99–107.

Biedermann T., Zimmermann S., Himmelrich H. *et al.* (2001) IL-4 instructs TH1 responses and resistance to *Leishmania major* in susceptible BALB/c mice. *Nat. Immunol.* **2**, 1054–1060.

Binah O. (2002) Cytotoxic lymphocytes and cardiac electrophysiology. *J. Mol. Cell. Cardiol.* **34**, 1147–1161.

Cordeiro F.D., Martins-Filho O.A., Costa Rocha M.O. *et al.* (2001) Anti-*Trypanosoma cruzi* immunoglobulin G1 can be a useful tool for diagnosis and prognosis of human Chagas disease. *Clin. Diag. Lab. Immunol.* **8**, 112–118.

Costa G.C., Rocha M.O., Moreira P.R. *et al.* (2009) Functional IL-10 gene polymorphism is associated with Chagas disease cardiomyopathy. *J. Infect. Dis.* **199**, 451–454.

Cummings K.L. & Tarleton R.L. (2004) Inducible nitric oxide synthase is not essential for control of *Trypanosoma cruzi* infection in mice. *Infect. Immun.* **72**, 4081–4089.

Federici E.E., Abelmann W.H., Neva F.A. (1964) Chronic and progressive myocarditis in C3H mice infected with *Trypanosoma cruzi*. *Am. J. Trop. Med. Hyg.* **13**, 272–280.

Feng Q., Lu X., Jones D.L., Shen J., Arnold J.M. (2001) Increased inducible nitric oxide synthase expression contributes to myocardial dysfunction and higher mortality after myocardial infarction in mice. *Circulation* **104**, 700–704.

Fichera L.E., Albareda M.C., Laucella A.S., Postan M. (2004) Intracellular growth of *Trypanosoma cruzi* in cardiac myocytes is inhibited by cytokine-induced nitric oxide release. *Infect. Immun.* **72**, 359–363.

Foote L.C., Howard R.G., Marshak-Rothstein A., Rothstein T.L. (1996) IL-4 induces Fas resistance in B cells. *J. Immunol.* **157**, 2749–2753.

Garcia S., Ramos C.O., Senra J.F.V. *et al.* (2005) Treatment with benznidazole during the chronic phase of experimental Chagas' disease decreases cardiac alterations. *Int. J. Antimicrob. Agents* **49**, 1521–1528.

Gomes J.A., Bahia-Oliveira L.M., Rocha M.O. *et al.* (2003) Evidence that development of severe cardiomyopathy in human Chagas' disease is due to a Th1-specific immune response. *Infect. Immun.* **71**, 1185–1193.

Henriques-Pons A., Oliveira G.M., Paiva M.M. *et al.* (2002) Evidence for a perforin-mediated mechanism controlling cardiac inflammation in *Trypanosoma cruzi* infection. *Int. J. Exp. Pathol.* **83**, 67–79.

Higuchi M.L., Reis M.M., Aiello V.D. *et al.* (1997) Association of an increase in $CD8^+$ T cells with the presence of *Trypanosoma cruzi* antigens in chronic, human chagasic myocarditis. *Am. J. Trop. Med. Hyg.* **56**, 485–489.

Higuchi M.L., Benvenuti L.A., Reis M.M., Metzger M. (2003) Pathophysiology of the heart in Chagas' disease: current status and new developments. *Cardiovasc. Res.* **60**, 96–107.

Huang H., Chan J., Wittner M. *et al.* (1999) Expression of cardiac cytokines and inducible form of nitric oxide synthase (NOS2) in *Trypanosoma cruzi*-infected mice. *J. Mol. Cell. Cardiol.* **31**, 75–88.

d'Imperio Lima M.R., Eisen H., Minoprio P., Joskowicz M., Coutinho A. (1986) Persistence of polyclonal B cell activation with undetectable parasitemia in late stages of experimental Chagas' disease. *J. Immunol.* **137**, 353–356.

Kierszenbaum F. (2005) Where do we stand on the autoimmunity hypothesis of Chagas disease? *Trends Parasitol.* **21**, 513–516.

Kumar S. & Tarleton R.L. (1998) The relative contribution of antibody production and $CD8^+$ T cell function to immune control of *Trypanosoma cruzi*. *Parasite Immunol.* **20**, 207–216.

Kumar S. & Tarleton R.L. (2001) Antigen-specific Th1 but not Th2 cells provide protection from lethal *Trypanosoma cruzi* infection in mice. *J. Immunol.* **166**, 4596–4603.

Lannes-Vieira J. (2003) *Trypanosoma cruzi*-elicited $CD8^+$ T cell-mediated myocarditis: chemokine receptors and adhesion molecules as potential therapeutic targets to control chronic inflammation? *Mem. Inst. Oswaldo Cruz* **98**, 299–304.

Laucella S.A., Postan M., Martin D. *et al.* (2004) Frequency of interferon-gamma-producing T cells specific for *Trypanosoma cruzi* inversely correlates with disease severity in chronic human Chagas disease. *J. Infect. Dis.* **189**, 909–918.

Machado F.S., Martins G.A., Aliberti J.C. *et al.* (2000) *Trypanosoma cruzi*-infected cardiomyocytes produce chemokines and cytokines that trigger potent nitric oxide-dependent trypanocidal activity. *Circulation* **102**, 3003–3008.

Marin-Neto J.A., Cunha-Neto E., Maciel B.C., Simoes M.V. (2007) Pathogenesis of chronic Chagas heart disease. *Circulation* **115**, 1109–1123.

Marino A.P., Silva A.A., dos Santos P.V. *et al.* (2004) Regulated on activation, normal T cell expressed and secreted (RANTES) antagonist (Met-RANTES) controls the early phase of *Trypanosoma cruzi*-elicited myocarditis. *Circulation* **110**, 1443–1449.

Martin D. & Tarleton R. (2004) Generation, specificity, and function of CD8+ T cells in *Trypanosoma cruzi* infection. *Immunol. Rev.* **201**, 304–317.

Medeiros G.A., Silverio J.C., Marino A.P. *et al.* (2009) Treatment of chronically *Trypanosoma cruzi*-infected mice with a CCR1/CCR5 antagonist (Met-RANTES) results in amelioration of cardiac tissue damage. *Microbes Infect.* **11**, 264–273.

Michailowsky V., Silva N.M., Rocha C.D. *et al.* (2001) Pivotal role of interleukin-12 and interferon-γ axis in controlling tissue parasitism and inflammation in the heart and central nervous system during *Trypanosoma cruzi* infection. *Am. J. Pathol.* **159**, 1723–1733.

Michailowsky V., Luhrs K., Rocha M.O. *et al.* (2003) Humoral and cellular immune responses to *Trypanosoma cruzi*-derived paraflagellar rod proteins in patients with Chagas' disease. *Infect. Immun.* **6**, 3165–3171.

Miranda K.M., Espey M.G., Wink D.A. (2001) A rapid, simple spectrophotometric method for simultaneous detection of nitrate and nitrite. *Nitric Oxide* **5**, 62–71.

Mitchell G.F., Jeron A., Koren G. (1998) Measurement of heart rate and Q–T interval in the conscious mouse. *Am. J. Physiol.* **274**, H747–H751.

Miyahira Y., Murata K., Rodriguez D. *et al.* (1995) Quantification of antigen specific CD8+ T cells using ELISPOT assay. *J. Immunol. Methods* **181**, 145–154.

Muller U., Sobek V., Balkow S. *et al.* (2003) Concerted action of perforin and granzymes is critical for the elimination of *Trypanosoma cruzi* from mouse tissue, but prevention of

early host death is in addition dependent on the Fas/FasL pathway. *Eur. J. Immunol.* **33**, 70–78.

Nickel S.P. & Sharma D. (2000) *Trypanosoma cruzi*: roles for perforin-dependent and perforin-independent immune mechanisms in acute resistence. *Exp. Parasit.* **94**, 207–216.

Perez-Fuentes R., Guegan J.F., Barnabe C. *et al.* (2003) Severity of chronic Chagas disease is associated with cytokine/antioxidant imbalance in chronically infected individuals. *Int. J. Parasitol.* **33**, 293–299.

Pipkin M.E. & Lieberman J. (2007) Delivering the kiss of death: progress on understanding how perforin works. *Curr. Opin. Immunol.* **19**, 301–308.

Reis D.D., Jones E.M., Tostes S. Jr. *et al.* (1993) Characterization of inflammatory infiltrates in chronic chagasic myocardial lesions: presence of tumor necrosis factor-alpha+ cells and dominance of granzyme A+, CD8+ lymphocytes. *Am. J. Trop. Med. Hyg.* **48**, 637–644.

Reis M.M., Higuchi M.L., Benvenuti L.A. *et al.* (1997) An *in situ* quantitaive immunohistochemical study of cytokines and IL-2R+ in chronic human chagasic myocarditi: correlation with the presence of myocardila *Trypanosoma cruzi* antigens. *Clin. Immunol. Immunopathol.* **83**, 165–172.

Saeftel M., Fleischer B., Hoerauf A. (2001) Stage-dependent role of nitric oxide in control of *Trypanosoma cruzi* infection. *Infect. Immun.* **69**, 2252–2259.

Sambhara S., Switzer I., Kurichh A. *et al.* (1998) Enhanced antibody and cytokine responses to influenza viral antigens in perforin-deficient mice. *Cell. Immunol.* **187**, 13–18.

Sandberg J.K., Fast N.M., Nixon D.F. (2001) Functional heterogeneity of cytokines and cytolytic effector molecules in human CD8+ T lymphocytes. *J. Immunol.* **167**, 181–187.

dos Santos P.V., Roffe E., Santiago H.C. *et al.* (2001) Prevalence of $CD8^+\alpha$ T cells in *Trypanosoma cruzi*-elicited myocarditis is associated with acquisition of $CD62L^{Low}LFA\text{-}1^{High}VLA\text{-}4^{High}$ activation phenotype and expression of IFN-γ-inducible adhesion and chemoattractant molecules. *Microbes Infect.* **3**, 971–984.

Severs N.J., Dupont E., Thomas N. *et al.* (2006) Alterations in cardiac connexin expression in cardiomyopathies. *Adv. Cardiol.* **42**, 228–242.

Silva J.S., Machado F.S., Martins G.A. (2003) The role of nitric oxide in the pathogenesis of Chagas disease. *Front. Biosci.* **8**, s314–s325.

de Souza A.P., Olivieri B.P., de Castro S.L., Araújo-Jorge T.C. (2000) Enzymatic markers of heart lesion in mice infected with *Trypanosoma cruzi* and submitted to benznidazole chemotherapy. *Parasitol. Res.* **86**, 800–808.

Tzelepis F., Persechini P.M., Rodrigues M.M. (2007) Modulation of CD4+ T cell-dependent specific cytotoxic CD8+ T cells differentiation and proliferation by the timing of increase in the pathogen load. *PLoS ONE* **2**, e393, 1–9.

Walsh C.M., Matloubian M., Liu C.C. *et al.* (1994) Immune function in mice lacking the perforin gene. *Proc. Natl. Acad. Sci. USA* **91**, 10854–10858.

Wirth J.J., Kierszenbaum F., Zlotnik A. (1989) Effects of IL-4 on macrophage functions: increased uptake and killing of a protozoan parasite (*Trypanosoma cruzi*). *Immunology* **66**, 296–301.

